forests

MDPI

Article

Anatomical Features and Its Radial Variations among Different *Catalpa bungei* Clones

Yamei Liu, Liang Zhou, Yingqi Zhu and Shengquan Liu *

Key Lab of State Forest and Grassland Administration on "Wood Quality Improvement & High Efficient Utilization", School of Forestry & Landscape Architecture, Anhui Agricultural University, Hefei 230036, China; liuyamei3980@126.com (Y.L.); mcyjs1@ahau.edu.cn (L.Z.); zhu123321dajuan@163.com (Y.Z.)
* Correspondence: liusq@ahau.edu.cn; Tel.: +86-0551-65786261

Received: 3 July 2020; Accepted: 27 July 2020; Published: 29 July 2020

Abstract: Research highlights: Annual wood anatomy (xylem) aids our understanding of mature wood formation and the growth strategies of trees. Background and Objectives: *Catalpa bungei* is an important native species in China that produces excellent quality wood. Herein, we clarified the effects of the genetic origin and cambial age on the anatomical characteristics of *C. bungei* wood. Materials and Methods: Six new 13-year-old *C. bungei* clones: '1-1' (n trees = 3), '1-3' (n trees = 3), '2-7' (n trees = 3), '2-8' (n trees = 3), '8-1' (n trees = 4), and '9-1' (n trees = 3) were removed for study from a plantation in Tianshui City, Gansu province, China. Xylem features were observed and the anatomical variables were manually measured via image analysis on (macro- micro-, and ultra-) features cut from radial increments of earlywood and latewood sampled at breast height. Results: Between the age of 1 and 2 years, wood was diffuse-porous; between the age of 3 and 9 years, wood was semi-ring-porous; and between the age of 10 and 13 years, wood was ring-porous. The effect of clones on anatomical characteristics was significant except for the microfibril angle in latewood and ring width. The transition between juvenile and mature wood was between 7 and 8 years based on patterns of radial variation in fiber length (earlywood) and microfibril angle. From the pith to the bark, fiber length, double wall thickness, fiber wall: lumen ratio, vessel diameter in earlywood, proportion of vessel in earlywood, and axial parenchyma in latewood increased significantly, whereas ring width, earlywood vessels, and the proportion of fiber decreased significantly. In addition, other features, such as vessel length, microfibril angle, and ray proportion, did not differ significantly from the pith to the bark. Conclusions: Breeding program must consider both clone and cambial age to improve the economic profitability of wood production.

Keywords: *Catalpa bungei*; clone; wood anatomy; fiber; vessel; earlywood; latewood; radial variation

1. Introduction

Catalpa bungei is a woody plant belonging to the genus *Catalpa*, from the Bignoniaceae family [1], commonly used to make furniture, coffins, musical instruments, and boats in ancient China (since 600 BC) for its high dimensional stability, resistance to deterioration, and mechanical performance [2,3]. Because natural plantations of *C. bungei* have decreased sharply in their abundance over the last century and are now protected, the utilization of *C. bungei* in the wood industry has decreased over the last two decades. Fast-growing *C. bungei* plantations have become increasingly cultivated to address the competing needs of the demand for wood products and the protection of natural forest. Much work in plant husbandry has been conducted to select genotypes that can grow fast, adapt to growing in various habitats, and are resistant to damage inflicted by pathogens and herbivores. The selection of genotypes has been successful given that several clones of *C. bungei* planted in central and northern parts of China now show many of these desired properties [4–11]. Aside from the survival and growth

of trees, the quality and utilization potential of timber should be considered when selecting tree species for large plantation programs and reforestation projects [12,13]. However, the properties of the wood of new breeding clones of *C. bungei* have not been systematically investigated compared with other fast-growing plantation species in China, such as *Cunninghamias*, *Eucalypts*, and *Populus*.

The anatomical features of wood provide the structural basis for other wood properties and are also often used to evaluate wood quality [14–17]. The anatomical properties of wood are closely related to many internal and external factors affecting tree growth, such as genetic origin, cambial age, and silvicultural practices. Wood anatomical properties are under strong genetic control in *Populus* [18,19], *Eucalypts* [20,21], and *Cunninghamias* [22,23]. Furthermore, Pande et al. [24] reported significant inter-clonal variation in wood anatomical properties in *Dalbergia sissoo* Roxb. Luostarinen et al. [13] found that clones of Finnish Norway spruce significantly differed from each other in anatomical characteristics.

In addition to genetic origin, the growth age of trees, namely cambial age, has a significant effect on the microstructure of wood. Researchers have reported that vessel diameter, fiber length, fiber diameter, cell wall thickness, and vessel frequency all change as age increases [25–31]. The radial growth of wood xylem, which is produced by cambium, can be divided into juvenile wood and mature wood [32]. Some authors [33–35] have reported that the age of transition from juvenile to mature wood varies considerably among trees and regions within a forest stand and can depend on seed provenance, local environmental conditions, and genetic factors. Ferreira et al. [36] also verified that juvenile and mature wood zones were located between approximately 40 and 55 mm from the pith in *Hevea brasiliensis* based on the pattern of radial variation in fiber length. Palermo et al. [37] studied the radial anatomical characteristics of *Eucalyptus grandis* wood and found that the transition age between juvenile and mature wood occurred between the ages of 8 and 13. However, variation in the wood anatomical properties caused by genetic origin and cambial age in *C. bungei* have been examined by only a couple of studies [38,39] and the estimation of essential parameters for characterizing patterns of radial variation, such as the microfibril angle (MFA) and proportions of different tissues, is lacking in these published works. Thus, there is a need for increased and better-quality data to be collected on the wood properties of *C. bungei*. The hypotheses for this study was that there is a difference in anatomical properties among different clones and cambial ages. Six new 13-year-old *C. bungei* clones were studied to provide a systematic description of the anatomical properties of *C. bungei* wood. MFA, dimensions of fibers/vessels, and the proportions of different tissues were examined in detail. Furthermore, different radial variation patterns were induced and differences in parameters among clones were summarized. The objectives of this study were to investigate anatomical properties of six new *C. bunbei* clones in two studies as follows: (1) study the impact of the genetic origin on anatomical properties; (2) study the radial variations of anatomical properties and determine the transition age between juvenile and mature wood.

2. Materials and Methods

2.1. Study Site

The experimental site was located in a plantation in Maiji district, Tianshui City, Gansu province, China (34°06′–34°48′ N, 105°25′–106°43′ E). The climate is characterized by distinct dry sub-humid seasons with a monsoon influence. The average yearly temperature is 11 °C and rainfall is 600–800 mm. Peak rainfall occurs from May to September and the dry season is November to March; April and October are the transition months. Trees in the plantation were spaced with a 3 m × 3 m configuration. The plantation was a monoculture and the land was flat and near roads.

2.2. Plant Material and Data Collection

We used six *C. bungei* clones: ‘1-1’ (n trees = 3), ‘1-3’ (n trees = 3), ‘2-7’ (n trees = 3), ‘2-8’ (n trees = 3), ‘8-1’ (n trees = 4), and ‘9-1’ (n trees = 3). The sample trees were selected based on their large diameters at

breast height and the straightness of their stems showing no apparent defects. At the time of harvesting, the height (11.4 ± 1.5 m) and stem diameters (15.3 ± 2.2 cm) of trees were measured (Table 1), the north direction was also marked. The average height of trees was between 8.8 and 12.5 m, the average diameter at breast height was between 11.7 and 16.9 cm, height and DBH were the smallest in 1-3. A 3-cm-thick cross-sectional disc from each tree was sampled at breast height for further analyses of wood anatomy.

Table 1. Means and standard deviations (SD) in height and DBH of six *C. bungei* clones.

	1-1 *n* = 3	**1-3** *n* = 3	**2-7** *n* = 3	**2-8** *n* = 3	**8-1** *n* = 4	**9-1** *n* = 3
Age, years	13	13	13	13	13	13
Height, m	11.9 ± 1.6 ^{a}	8.8 ± 1.8 ^{b}	11.9 ± 0.1 ^{a}	11.6 ± 0.3 ^{a}	11.8 ± 0.6 ^{a}	12.5 ± 0.6 ^{a}
Diameter at breast height, cm	16.9 ± 1.9 ^{a}	11.7 ± 2.4 ^{b}	15.7 ± 1.2 ^{ab}	14.8 ± 0.6 ^{ab}	16.4 ± 1.8 ^{a}	15.9 ± 1.1 ^{ab}

Note: *n* is the number of trees within a clone. Statistical differences between clones are denoted using lowercase letters, with different letters corresponding to significant differences ($p < 0.05$). Diameter at breast height (bark included) was measured along the north-south direction. Different letters corresponding to significant differences, ANOVAs were followed by Tukey's tests at the 5% significance level to compare means using SPSS 19.0 software.

The samples for anatomical properties analyses were taken from the north side of each trunk so that the growth conditions of the studied wood were as similar as possible. Age was rechecked by counting the rings from the anatomical crosscuts at breast height; the length of strips of north side and annual ring width (mm) in the four directions (east, west, south, and north) was measured for each sample tree. Sapwood and heartwood were separated on the basis of color [40,41]. Growth rings were distinct; the boundary between earlywood (EW) and latewood (LW) was not distinct at the macroscopic scale. The unusual narrower rings occurred from years 10 to 13 in 1-3; it was difficult to distinguish the boundary of the last four rings with the naked eye. Observations of the wood features of *C. bungei* wood were made under a microscope.

2.3. Measurements of Anatomical Characteristics

For anatomical characterization, wood macerations were conducted using glacial acetic acid and 30% hydrogen peroxide (1:1 ratio) at 80 °C for 4 h. The macerated tissue was washed in running water until the tissue was free of all acid traces so that the lengths of the fibers and vessel elements could be determined. The fibers and vessel elements were observed using a depth of field microscope (Keyence VXH-600E, Keyence Corporation, Tokyo, Japan), and images were taken at 200× magnification for analysis. In total, 15 measurements were taken for vessel length and 50 measurements were taken for fiber length of both EW and LW. These measurements were carried out for each annual ring from the pith to the bark.

Wood cubes ($2 \times 2 \times 2$ cm^3) were prepared annually along radial positions from the pith to the bark. The wood blocks were softened by boiling in water with a microwave for approximately 15–20 min, transverse, radial and tangential microscopic sections (approximately 25–30 μm thick) were prepared with a rotary microtome Leica RM 2265 (Wetzlar, Germany). The sections were stained with safranin (5%) for approximately one minute, dehydrated with an ethanol series (50%, 70%, 80%, 90%, and 100%) for a few seconds, washed with 50% xylene and pure xylene, and mounted with a drop of Canada balsam. After drying, sections were observed using a light microscope (Nikon ECLIPSE Ni, Nikon Corporation, Tokyo, Japan) with a DS- Ri2 camera and Image NIS 5.10 software, and images were taken at 2× and 4× magnifications for analysis. ImageJ (National Institutes of Health, Bethesda, MD, USA) was used to analyze all images.

The Nikon microscope was used to measure the double thickness of the fiber wall. Fiber lumen diameter in the tangential direction was measured randomly by selecting 50 cells in each ring. Furthermore, the fiber diameter was calculated (double cell wall + lumen diameter). Fiber wall: lumen ratio was calculated using the double thickness of the cell wall and fiber lumen diameter. As vessels became rarer in LW, it became increasingly difficult to locate 50 vessel cells; in such cases, measurements

of vessel diameter were reduced to 30. In addition, the number (No.) of vessels was counted at 4× magnification for each ring per mm^2. The average vessel number was calculated from 20 vessels per slide.

The proportion of tissue types was calculated in the transverse section on 30 randomly selected areas using the NIS 5.10 image analysis system coupled to a Nikon microscope. A grid of 25-points was placed over each image and tissue types (i.e., fiber, axial parenchyma, vessel, and ray) were counted and converted into a percentage of the total area following Quilho et al. [14].

For scanning electron microscopy (SEM), 1-mm thick wood slices in the radial and tangential directions were prepared and oven-dried at 60 °C for 24 h. The slices were subsequently coated with gold at 15 mA in an anion sputter coater (KYKY SBC-12, KYKY, Ltd., Beijing, China) for 20 s and were observed via SEM (TESCAN VEGA 3 SBH, TESCAN, Ltd., Kohoutovice, Czech Republic) under a high vacuum (10 kV accelerate voltage, 10 mm or 15 mm working distance, SE detector).

The demarcations of the juvenile and mature wood regions were determined through a visual analysis of graphs obtained from the fiber length and MFA, as recommended by Zobel et al. [20], Mansfield et al. [42], Palermo et al. [37], Gorman et al. [43], and Dobrowolska et al. [44].

Wood slices with 1 mm (R) × 10 mm (T) × 30 mm (L) were prepared and equilibrated for 1 week in a constant temperature and humidity chamber where the temperature was 20 °C and the relative humidity was 65%. MFA was measured by X-ray diffraction (XD-3, Beijing Persee Instrument Co., Ltd., Beijing, China) with the following parameters: 36 kV voltage, 20 mA electricity, and 1.54 wavelength. The data were then calculated using the 0.6 T method [45] with Origin 2019b software.

2.4. Statistical Analyses

The means of anatomical properties were calculated from the individual samples and ANOVAs were performed using SPSS 19.0 software IBM (USA) to determine whether there were significant differences between clones. ANOVAs were followed by Tukey's tests at the 5% significance level to compare means. Variation in traits with cambial age was fitted with a multiple linear regression equation using Origin 2019b software (USA). Models of the regression curves were constructed using a 5% significance level. R square was also calculated to assess the robustness of the correlations.

Descriptive anatomical terminology followed the IAWA list of microscopic features for hardwood identification [46].

3. Results

3.1. Xylem Anatomical Features

The sapwood and heartwood of *C. bungei* was clearly distinguished (brightness value was 64.2 in sapwood and 62.3 in heartwood), as sapwood was light brown while heartwood was dark brown (Figure 1). Sapwood was narrow from 10 to 13 years and regular along the stem circumference. The length of strips (from pith to the bark) was different among clones; the length was longest in 8-1 and shortest in 1-3, indicating that the growth rate varied among clones.

Between the age of 1 and 2 years, the wood was diffuse-porous; between the age of 3 and 9 years, the wood was semi-ring-porous; and between the age of 10 and 13 years, the wood was ring-porous (Figure 2). The latewood percentage became smaller from the pith to bark. The vessels were solitary, in short radial multiples of 2–3 cells, in clusters common (more frequent in LW) and occasionally filled with thin-walled tyloses (Figure 3d). They were almost circular to oval in outline with an average tangential diameter of 148 μm (184 in EW and 105 in LW) and an average vessel element length of 278 μm (200 in EW and 378 in LW). The transition from EW to LW was gradual. Vessels occupied 18% (28% in EW and 9% in LW) of the ring area, corresponding to an average of 14 (12 in EW and 19 in LW) vessels/mm^2.

Axial parenchyma made up approximately 9.4% (10.2% in EW and 9.6% in LW) of the tissues. Vasicentric (Figure 2e), paratracheal-zonate parenchyma (Figure 2c,f) and axial parenchyma were not storied, and there were more than 10 cells per parenchyma strand.

Fibers represented approximately 63% (53 in EW and 71 in LW) of the wood cross-sectional area and were 851 µm (816 in EW and 886 in LW) in length, 18.6 µm (18.9 in EW and 18.4 in LW) in width, and 4.6 µm (4.1 in EW and 5.0 in LW) in double wall thickness.

Rays occupied 10% of the wood cross-sectional area. The rays were 2–3 cells wide (Figure 2f) and heterocellular with one row of upright and square marginal cells (Figure 3h).

Intervessel pits were alternates for *C. bungei* (Figure 3a–c). The average pit aperture width in LW was 3.78 µm (minute) (Figure 3e) compared with 5.17 µm (small) (Figure 3f) in EW. The deposition decreased from the pith to the bark, and the warty layers could be seen clearly (Figure 3e). Helical thickenings were present in the whole body of the vessel elements. Perforations were simple (Figure 3g).

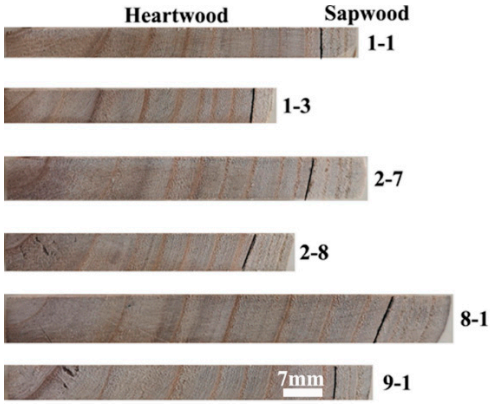

Figure 1. Xylem observations of six *C. bungei* clones. The cross-sectional surface was photographed under air-dried conditions.

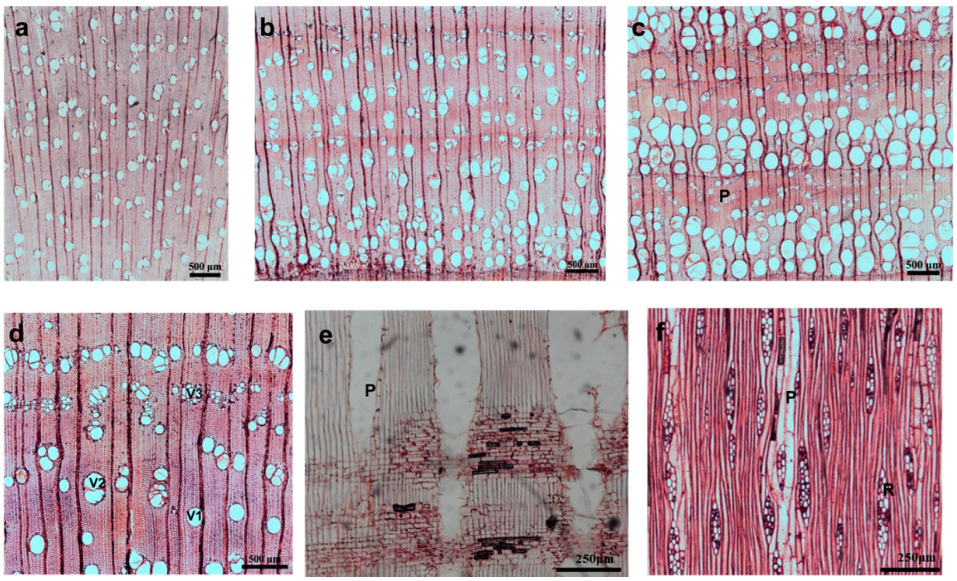

Figure 2. Sections of xylem in *C. bungei* in 1-1: (**a**) between the age of 1 and 2 years, wood was diffuse-porous; (**b**) between the age of 3 and 9 years, wood was semi-ring-porous, ring width was approximately 5 mm, and the latewood percentage was 80%; (**c**) between the age of 10 and 13 years, wood was ring-porous, ring width was approximately 2 mm, and the latewood percentage was 30%; axial parenchyma (P) with 5–15 cells per parenchyma strand; (**d**) vessels solitary (V1), radial multiples of 2–3 cells (V2), and clusters common (V3) in wood diffuse-porous; (**e**) radial section of the second year, vasicentric axial parenchyma (P); (**f**) tangential section of latewood areas from the 8th year, fusiform ray (R) width was 2–3 cells, axial parenchyma (P) in paratracheal-zonate.

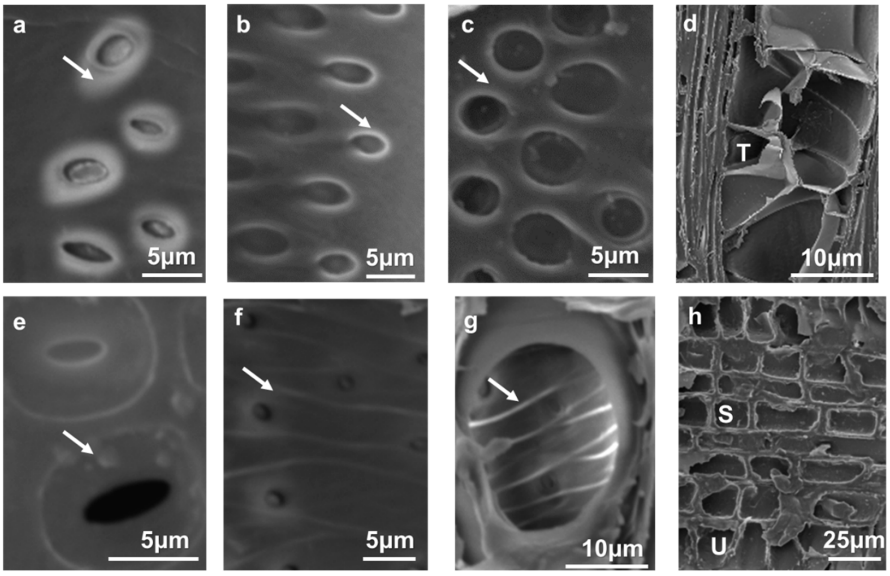

Figure 3. Scanning electron microscopy (SEM) photos of the radial and tangential sections of *C. bungei* in 1-1. (**a**) Intervessel pits with numerous depositions (arrow) in EW of the 2nd year; (**b**) intervessel pits with fewer depositions (arrow) in EW of the 7th year; (**c**) intervessel pits with rare depositions (arrow) in EW of the 12th year; (**d**) thin-walled tyloses in vessel elements; (**e**) warty layers in the pits (arrow) in EW of the 9th year; (**f**) the small pits in LW of the 9th year (arrow); (**g**) simple perforation plates and helical thickenings (arrow) in vessel elements; (**h**) ray cells heterocellular with one row of upright (U) and square marginal (S) cells.

3.2. Variation in Anatomical Characteristics Between Clones

Significant differences were found among the clones for all characteristics except annual ring width and MFA in LW (Table 2).

3.3. Radial Variation in Anatomical Characteristics

Each of the six clones showed the same pattern (Figure 4) of ring width which significantly decreasing with cambial age (R^2 = 0.89). From the pith to the eighth year, ring width decreased rapidly. After the eighth year, changes in ring width stabilized.

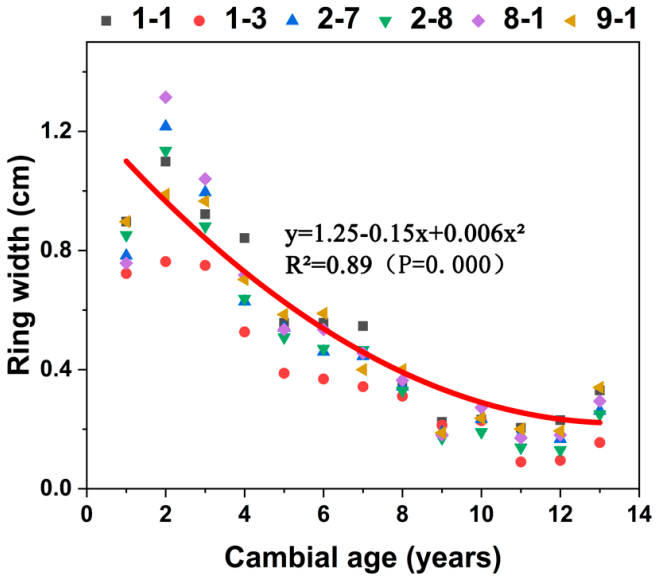

Figure 4. Average ring width of wood in six *C. bungei* clones versus cambial age.

Table 2. Means (M) and standard deviations (SD) of measured anatomical characteristics in six *C. bungei* clones.

Anatomical Characteristic		1-1			1-3			2-7			2-8			8-1			9-1		
		n	M ± SD	CV%	*n*	M ± SD	CV%	*n*	M ± SD	CV%	*n*	M ± SD	CV%	*n*	M ± SD	CV%	*n*	M ± SD	CV%
Ring width, cm		156	0.53 ± 0.33 ^{a}	62.3	132	0.43 ± 0.28 ^{a}	65.1	156	0.50 ± 0.36 ^{a}	72.0	156	0.47 ± 0.34 ^{a}	72.3	208	0.52 ± 0.37 ^{a}	71.2	156	0.51 ± 0.33 ^{a}	64.7
Fiber length, μm	EW	1800	851 ± 99.6 ^{a}	11.7	1600	830 ± 141.9 ^{b}	17.1	1800	828 ± 94.8 ^{b}	11.4	1800	757 ± 88.8 ^{c}	11.7	2350	857 ± 98.1 ^{a}	11.4	1749	758 ± 78.6 ^{c}	10.4
	LW	1850	879 ± 91.8 ^{c}	10.5	1600	880 ± 129.7 ^{c}	14.7	1800	879 ± 74.8 ^{c}	8.5	1800	834 ± 86.1 ^{d}	10.3	2499	934 ± 107.1 ^{a}	11.5	1850	890 ± 110.4 ^{b}	12.4
Fiber diameter, μm	EW	1881	18.5 ± 4.5 ^{b}	24.0	1764	18.5 ± 3.9 ^{b}	21.0	1794	21.3 ± 5.4 ^{a}	25.3	1822	18.7 ± 5.3 ^{b}	28.3	2452	18.3 ± 4.7 ^{b}	25.7	1791	18.6 ± 5.5 ^{b}	29.6
	LW	1887	17.9 ± 4.3 ^{c}	24.0	1736	18.6 ± 3.4 ^{b}	18.3	1797	21.0 ± 5.5 ^{a}	26.2	1859	18.8 ± 9.7 ^{b}	51.6	2450	17.4 ± 3.9 ^{c}	22.4	1845	16.9 ± 4.5 ^{d}	26.6
double thickness of cell wall, μm	EW	1881	4.29 ± 1.0 ^{a}	23.2	1764	4.06 ± 1.1 ^{b}	26.8	1794	4.32 ± 1.3 ^{a}	30.2	1822	3.68 ± 1.0 ^{d}	27.0	2452	4.14 ± 1.0 ^{b}	24.3	1791	3.80 ± 0.9 ^{c}	23.7
	LW	1887	4.95 ± 1.0 ^{b}	20.2	1736	4.60 ± 1.0 ^{c}	21.7	1797	4.82 ± 1.3 ^{b}	27.0	1859	5.14 ± 2.6 ^{a}	50.6	2450	5.13 ± 1.0 ^{a}	19.5	1845	5.01 ± 0.9 ^{ab}	18.0
Fiber wall: lumen ratio	EW	1881	0.33 ± 0.1 ^{a}	40.3	1764	0.30 ± 0.1 ^{b}	39.3	1794	0.28 ± 0.1 ^{c}	42.0	1822	0.27 ± 0.1 ^{c}	43.6	2452	0.32 ± 0.1 ^{a}	47.1	1791	0.30 ± 0.1 ^{b}	48.6
	LW	1887	0.42 ± 0.1 ^{c}	23.8	1736	0.35 ± 0.1 ^{d}	28.6	1797	0.33 ± 0.1 ^{e}	30.3	1859	0.42 ± 0.2 ^{c}	47.6	2450	0.46 ± 0.2 ^{b}	43.5	1845	0.48 ± 0.2 ^{a}	41.7
MFA, °	EW	34	17.2 ± 3.7 ^{b}	21.5	27	17.6 ± 3.2 ^{b}	18.2	35	15.9 ± 2.2 ^{b}	13.8	35	18.6 ± 4.1 ^{ab}	22.0	47	18.1 ± 4.9 ^{ab}	27.1	35	20.4 ± 4.7 ^{a}	23.0
	LW	36	16.0 ± 2.9 ^{a}	18.1	27	15.1 ± 2.2 ^{a}	14.6	36	14.9 ± 3.0 ^{a}	20.1	36	16.1 ± 3.5 ^{a}	21.7	48	15.9 ± 2.9 ^{a}	18.2	36	15.2 ± 2.5 ^{a}	16.4
Vessel length, μm	EW	720	206 ± 92.0 ^{b}	44.7	640	219 ± 59.7 ^{a}	27.3	717	214 ± 97.4 ^{ab}	45.6	722	185 ± 49.3 ^{c}	26.6	960	188 ± 42.9 ^{c}	22.9	709	195 ± 39.3 ^{c}	20.2
	LW	555	389 ± 232.2 ^{ab}	59.7	480	408 ± 232.1 ^{a}	56.9	540	388 ± 189.2 ^{ab}	48.7	555	362 ± 190.6 ^{bc}	52.6	780	334 ± 184.0 ^{c}	55.1	570	408 ± 188.9 ^{a}	46.3
Vessel lumen diameter, μm	EW	2160	180 ± 48.2 ^{c}	26.8	1980	168 ± 51.6 ^{d}	30.7	2140	203 ± 56.6 ^{a}	27.9	2160	187 ± 58.0 ^{b}	31.1	2880	181 ± 54.8 ^{c}	30.4	2100	187 ± 57.2 ^{b}	30.6
	LW	2010	108 ± 33.9 ^{a}	31.1	1304	105 ± 31.5 ^{b}	30.1	1560	106 ± 33.5 ^{ab}	31.5	1140	109 ± 31.4 ^{a}	28.9	1680	105 ± 32.1 ^{b}	30.7	1560	100 ± 31.7 ^{c}	31.8
No. of vessels, no/mm^2	EW	620	13 ± 3.3 ^{b}	26.5	580	12 ± 3.4 ^{bc}	27.7	717	10 ± 4.4 ^{d}	43.8	660	15 ± 8.1 ^{a}	54.6	920	12 ± 4.5 ^{c}	38.6	700	11 ± 4.3 ^{d}	40.2
	LW	509	16 ± 5.9 ^{c}	35.9	400	17 ± 7.4 ^{bc}	43.2	720	23 ± 13.0 ^{a}	55.9	478	23 ± 10.7 ^{a}	46.7	740	15 ± 6.6 ^{d}	45.3	580	18 ± 9.5 ^{b}	51.2
Proportion of fiber, %	EW	1082	47.2 ± 11.5 ^{e}	24.4	988	49.5 ± 13.7 ^{d}	27.6	1080	48.1 ± 11.5 ^{de}	23.9	1050	53.7 ± 11.1 ^{c}	20.7	1440	58.7 ± 12.8 ^{a}	21.8	1056	55.9 ± 12.5 ^{b}	22.3
	LW	1019	67.3 ± 10.6 ^{d}	15.8	780	67.2 ± 10.1 ^{d}	15.0	1078	71.0 ± 8.2 ^{c}	11.6	810	71.0 ± 7.4 ^{c}	10.4	1140	77.1 ± 7.7 ^{a}	10.0	779	71.9 ± 30.9 ^{b}	43.0
Proportion of vessel, %	EW	1082	31.4 ± 10.1 ^{a}	32.3	988	28.1 ± 12.6 ^{b}	44.6	1080	30.4 ± 10.0 ^{a}	32.9	1050	27.0 ± 10.1 ^{bc}	37.4	1440	25.4 ± 11.3 ^{d}	44.6	1056	25.8 ± 10.3 ^{cd}	40.1
	LW	1019	10.3 ± 6.6 ^{ab}	64.3	780	10.6 ± 7.4 ^{a}	70.3	1078	6.8 ± 5.3 ^{d}	77.9	810	10.6 ± 5.2 ^{a}	48.9	1140	8.4 ± 4.9 ^{c}	58.1	779	9.6 ± 5.1 ^{b}	53.4
Proportion of ray, %	EW	1082	9.4 ± 5.3 ^{bc}	56.2	988	9.7 ± 5.3 ^{bc}	55.0	1080	10.0 ± 5.2 ^{b}	51.5	1050	9.3 ± 5.6 ^{c}	60.1	1440	7.4 ± 4.8 ^{d}	64.7	1056	10.9 ± 5.6 ^{a}	51.0
	LW	1019	9.6 ± 6.6 ^{c}	69.0	780	9.6 ± 5.5 ^{c}	57.3	1078	9.3 ± 5.1 ^{c}	54.7	810	10.7 ± 5.6 ^{b}	51.9	1140	8.9 ± 4.9 ^{c}	55.5	779	11.9 ± 5.4 ^{a}	45.2
Proportion of axial parenchyma, %	EW	1082	12.1 ± 5.9 ^{ab}	48.8	988	12.7 ± 6.8 ^{a}	53.6	1080	11.5 ± 6.0 ^{b}	52.3	1050	9.9 ± 5.3 ^{c}	52.9	1440	8.5 ± 5.0 ^{d}	58.6	1056	7.4 ± 5.2 ^{e}	70.7
	LW	1019	12.7 ± 7.0 ^{a}	54.7	780	12.6 ± 6.5 ^{a}	51.7	1078	12.9 ± 6.6 ^{a}	51.3	810	7.7 ± 4.4 ^{b}	57.8	1140	5.6 ± 4.1 ^{c}	73.4	779	5.4 ± 3.6 ^{c}	66.6

Note: EW, earlywood; LW, latewood; MFA, microfibril angle; *n*, number of samples; CV%, coefficient of variation. Statistical differences between clones are denoted using lowercase letters, with different letters corresponding to significant differences ($p < 0.05$). Different letters corresponding to significant differences, ANOVAs were followed by Tukey's tests at the 5% significance level to compare means using SPSS 19.0 software.

In the radial direction, EW fiber length showed a rapid and nearly linear increase (R^2 = 0.88) until the age of 7–8 years after the pith (Figure 5). From years 7 to 8 to the periphery, the rate of increase in fiber length decreased and tended to stabilize to a constant value. In LW, fiber length showed slight increases (R^2 = 0.35) from the pith to the bark, and there was no distinct demarcation between juvenile and mature wood.

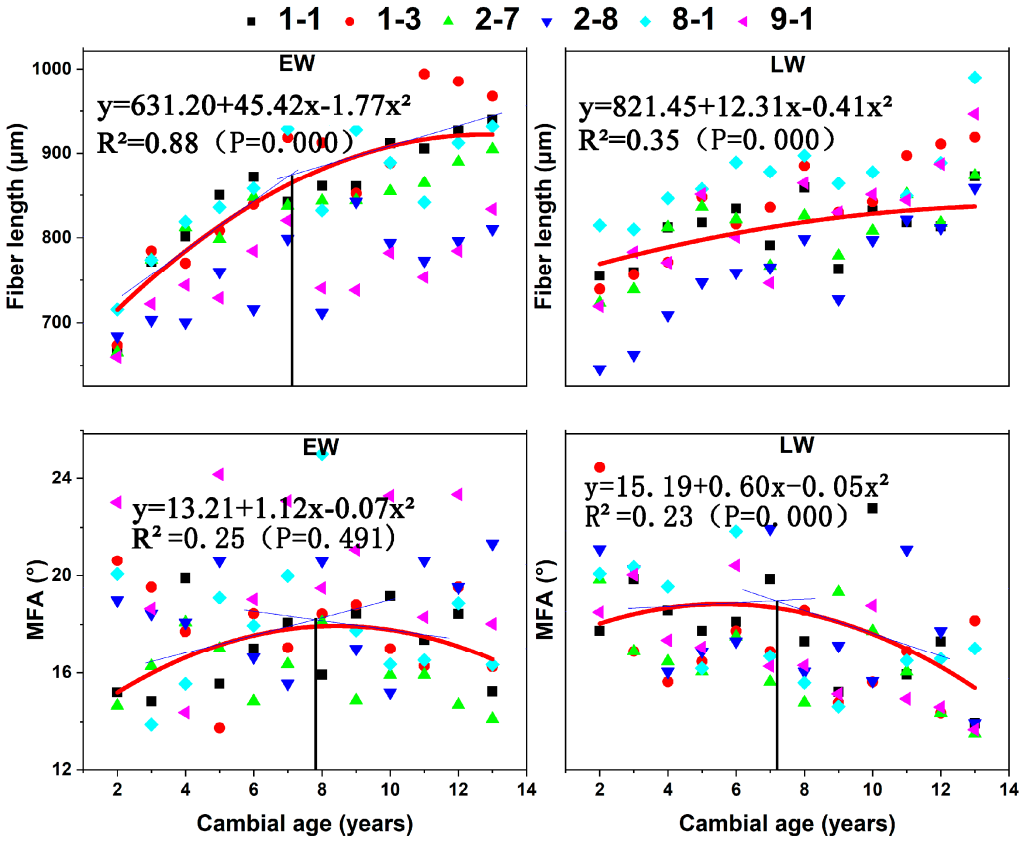

Figure 5. Variation in earlywood (EW) and latewood (LW) in fiber length and microfibril angle (MFA) revealed the demarcation between the juvenile and mature wood zones from six *C. bungei* clones. The demarcation between juvenile and mature wood zones was calculated through tangent intersection according to the multiple linear regression curves.

MFA of EW and LW showed similar trends from the pith to the bark. In EW and LW, the angle increased from the pith until the 8th year, and then the angle decreased to the periphery. The effect of age on MFA was not significant in EW.

The demarcation between juvenile and mature wood based on fiber length and MFA was calculated by two-segment regression. The juvenile wood zone consisted of the first 7 to 8 growth rings. Juvenile wood width ranged between 4.2 and 5.8 cm, and the proportion of juvenile wood ranged between 82.7 and 88.3% (Table 3). The juvenile wood widths were significantly different among clones, but the effect of clone on the proportion of juvenile wood was not significant.

Table 3. Means and standard deviations (SD) in six *C. bungei* clones.

	1-1 n = 3	1-3 n = 3	2-7 n = 3	2-8 n = 3	8-1 n = 4	9-1 n = 3
Juvenile wood width, cm	5.8 ± 0.8 ^{a}	4.2 ± 0.9 ^{b}	5.4 ± 0.4 ^{ab}	5.3 ± 0.1 ^{ab}	5.7 ± 0.6 ^{ab}	5.5 ± 0.2 ^{ab}
Proportion of juvenile wood, %	82.7 ± 3.7 ^{a}	88.3 ± 1.9 ^{a}	84.0 ± 2.9 ^{a}	85.8 ± 2.0 ^{a}	83.8 ± 2.4 ^{a}	82.7 ± 2.6 ^{a}

Note: n is the number of trees within a clone. Statistical differences between clones were denoted using lowercase letters, with different letters corresponding to significant differences ($p < 0.05$). Different letters corresponding to significant differences, ANOVAs were followed by Tukey's tests at the 5% significance level to compare means using SPSS 19.0 software.

The fiber diameter of LW significantly decreased with cambial age until the 8th year and then increased, whereas diameter in EW was largely independent of cambial age (R^2 = 0.08) (Figure 6).

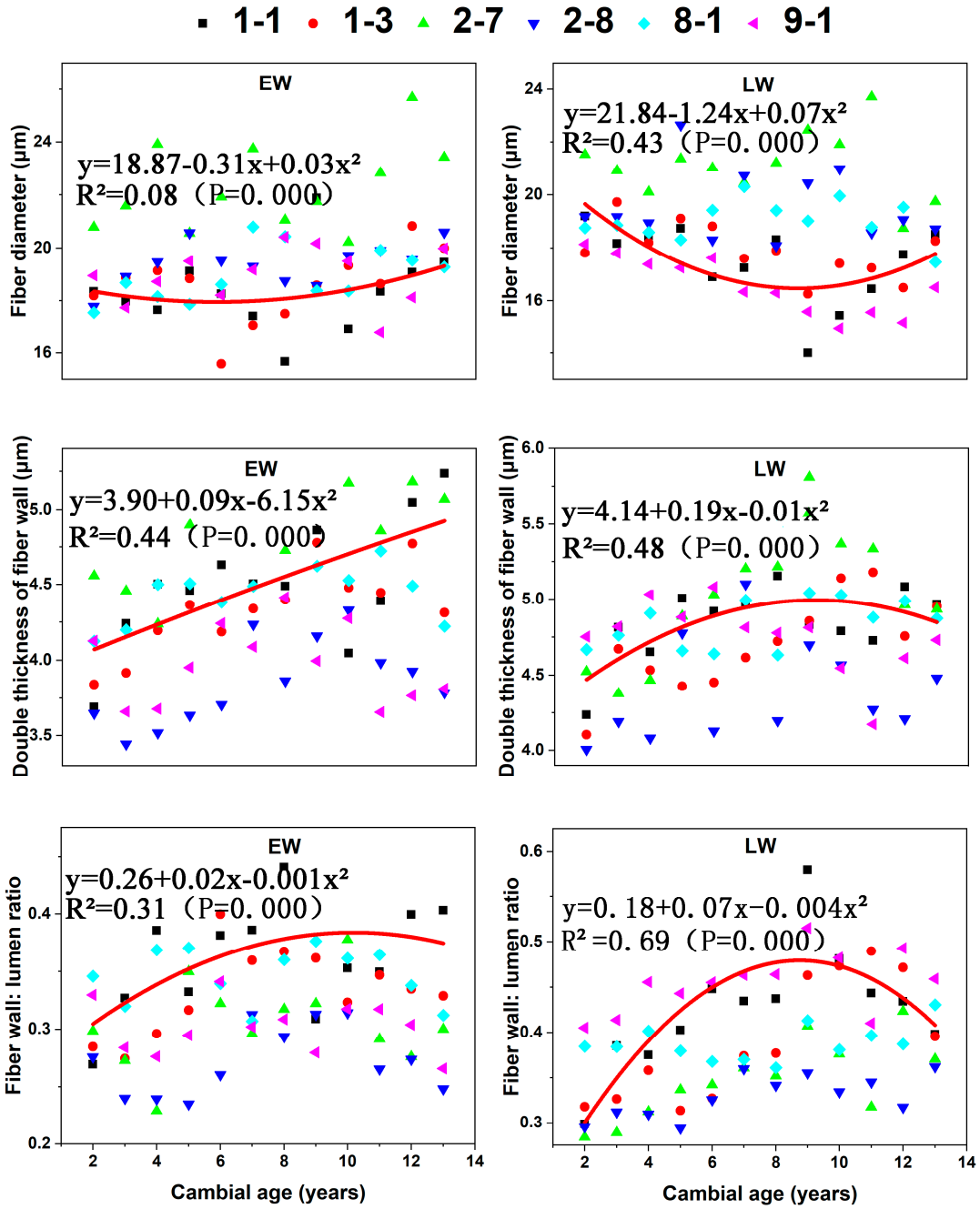

Figure 6. The fiber characters in both earlywood (EW) and latewood (LW): fiber diameter, double thickness of fiber wall, and fiber wall: lumen ratio for the six *C. bungei* clones versus cambial age.

There were pronounced effects of age on the double thickness of cell wall (R^2 = 0.44 for EW and 0.48 for LW). Thickness significantly increased with cambial age in EW. In contrast, thickness increased until the eighth year and then remained stable in LW. The fiber wall: lumen ratio increased from the pith to the eighth year and then remained stable in EW and decreased from the eighth year to the bark in LW. Radial variation in LW (R^2 = 0.69) was more pronounced than in EW (R^2 = 0.31).

Vessel length in LW, vessel diameter in EW, and the number of vessels in EW varied significantly from the pith to the bark (Figure 7). Variation in vessel length in EW, vessel diameter in LW, and the number of vessels in LW was not radially significant. Variation in the radial pattern was characterized

by increases in vessel diameter in EW with cambial age, vessel length increases and then decreases in LW, and a decreasing trend in the No. of vessels of EW.

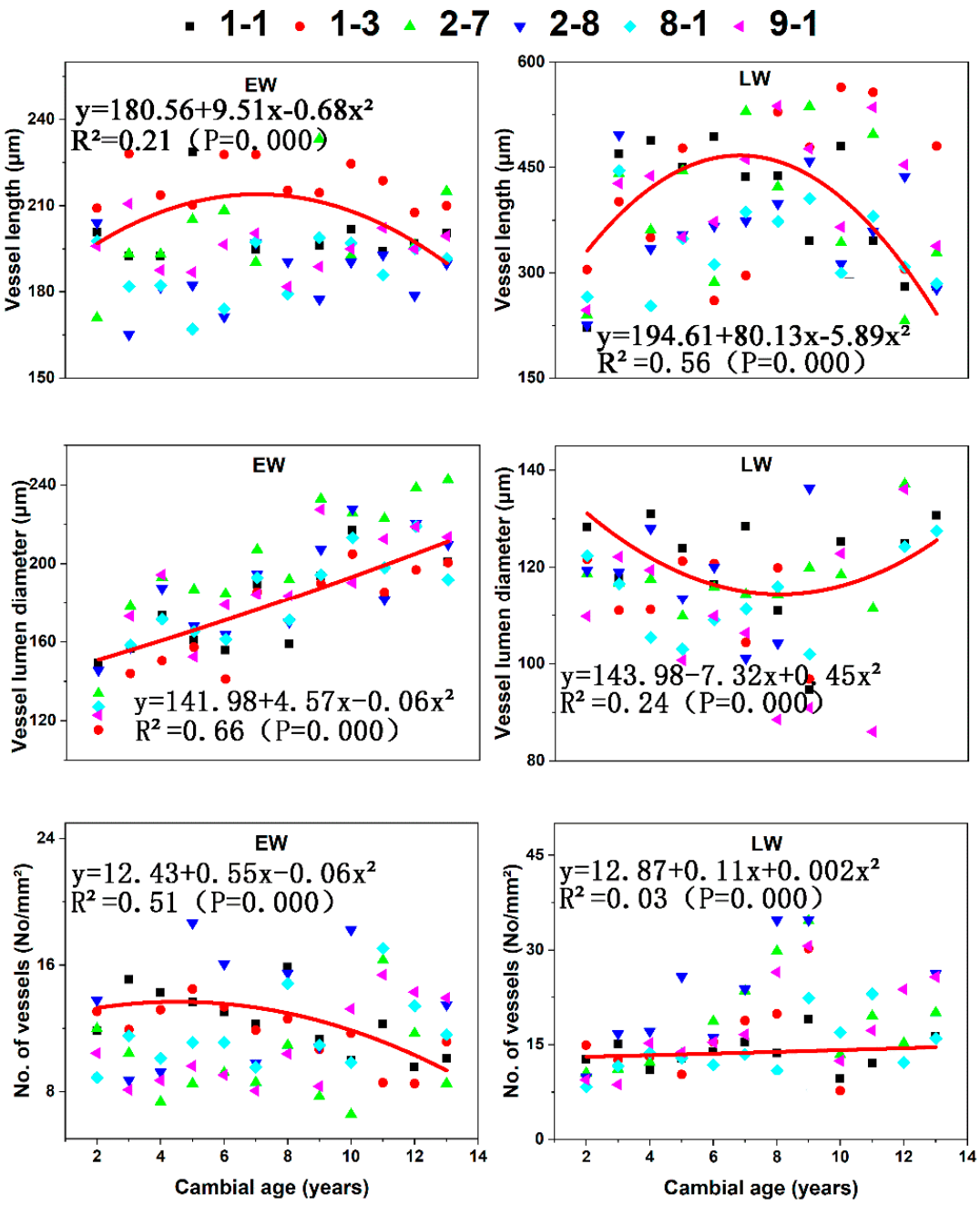

Figure 7. Vessel characters of both earlywood (EW) and latewood (LW): vessel length, vessel diameter, and the number of vessels for the six *C. bungei* clones versus cambial age.

Proportion of fiber in both EW and LW decreased significantly until the eighth year (Figure 8). Proportion of vessel increased with cambial age in EW until the eighth year and then stabilized. Proportion of axial parenchyma in LW also increased until the eighth year and then stabilized similar to the pattern observed for the proportion of vessel. Overall, the proportion of ray, proportion of vessel in LW, and proportion of axial parenchyma in EW did not change radially.

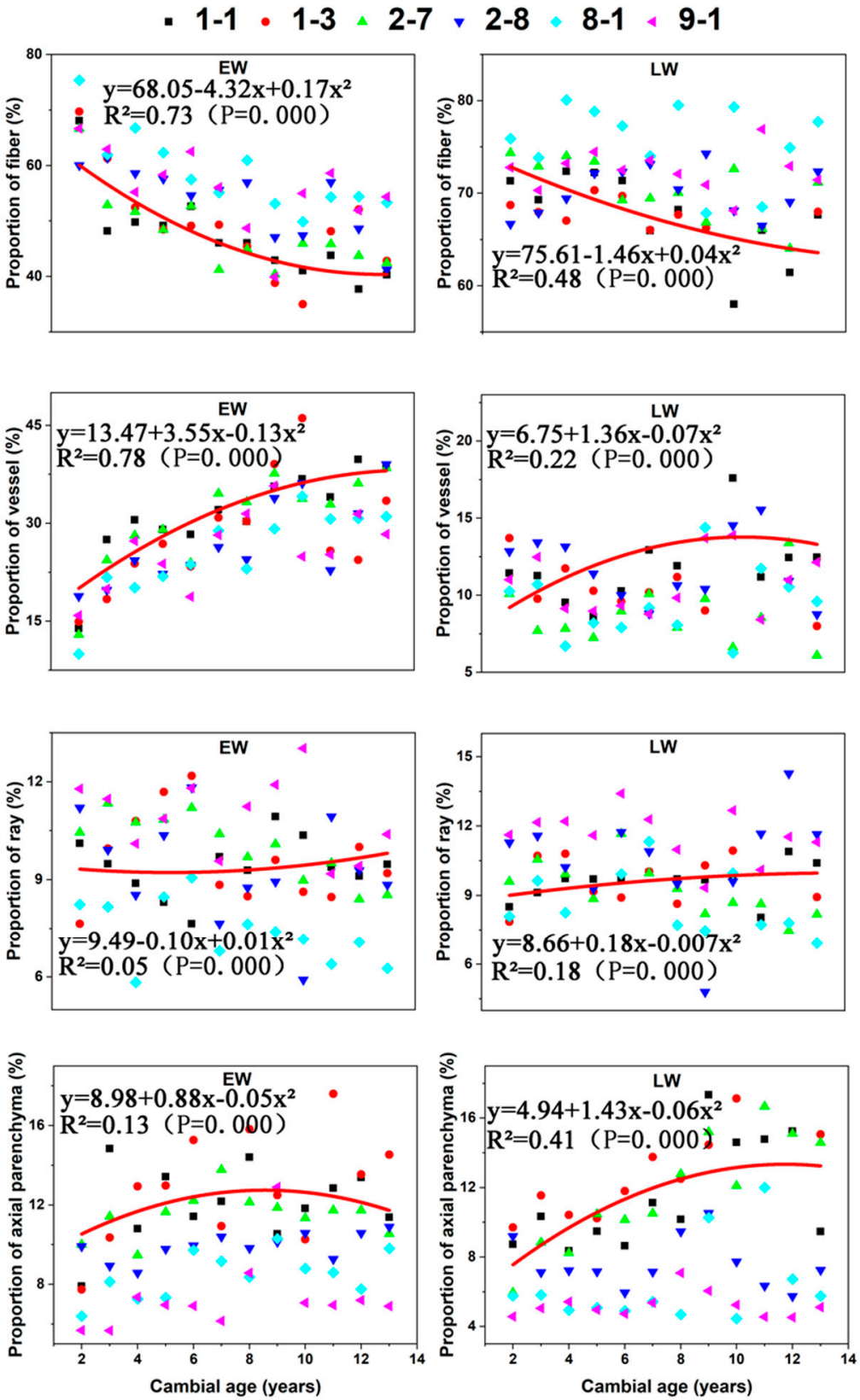

Figure 8. The proportion of different tissues in earlywood (EW) and latewood (LW): proportion of fiber, proportion of vessel, proportion of ray, and proportion of axial parenchyma for the six *C. bungei* clones versus cambial age.

4. Discussion

4.1. Xylem Anatomical Features

The wood anatomical features changed along radial direction, which was consistent with the proposed hypotheses. Woody angiosperms are widely divergent in the cellular makeup of their xylem [47]. Ring-porous wood is usually widespread in temperate climates [48]. According to our study, there were three different types of radial porous distributions: diffuse-porous, semi-ring-porous, and ring-porous. These results were not consistent with those of Li et al. [39], who studied mature *C. bungei* and concluded that *C. bungei* was largely a ring-porous tree species. This difference may stem from the fact that the most obvious characteristics of immature xylem consisted of the gradual transition between EW and LW [49].

Sapwood and heartwood can be clearly distinguished based on their color and the presence of tyloses [50]. Some authors [51,52] have reported that heartwood permeability is low, suggesting that tyloses or other deposits obstruct vessels. In our study, the observation of decreasing amounts of deposits from heartwood to sapwood in *C. bungei* was consistent with the observations of previous studies. Tyloses, warty layers, and cell walls with helical thickenings tend to be more effective structures for maintaining moisture and thereafter resist microorganisms and embolism [53].

4.2. Variation in Anatomical Characteristics between Clones

The effect of clones on most of the anatomical characteristics was significant (Table 2), which verified our hypothesis. The six clones in this study were selected by clonal breeding, meaning that the goal of this previous selection was to increase the commercial production of wood. With the development of the wood industry, increasingly competitive market pressures are encouraging forest industries to shift their focus from wood volume to wood quality [54]. Wood anatomical traits related to wood quality include the proportion of juvenile wood, wood density, fiber length, and MFA. These anatomical traits underly the physical and mechanical properties of wood, such as its shrinkage behavior, bending, stiffness, and strength [55]. For example, juvenile wood is typically characterized as being less dimensionally stable and having weaker mechanical properties than mature wood [43]. The quality of fibers has a pronounced effect on wood strength and shrinkage [56,57]. The fiber wall: lumen ratio has a major effect on wood density [58,59]. Extractives in axial parenchyma commonly increase the resistance of wood to decay [60]. MFA has been shown to directly impact the shrinkage behavior and flexural properties of wood, and these changes can alter several physical and mechanical properties of wood [55,61–64].

In addition, these results were similar to those found by Ma et al. [38], who studied the wood properties of 11 three-year seedling trunks of *C. bungei* clones and showed that fiber length, fiber percentage, and vessel percentage were highly significantly different between clones with high repeatability and strong genetic control.

Some clones showed higher performance in terms of wood quality characters relative to others. For example, if fiber quality is considered, 8-1 was the best clone. Thus, selection of this clone may result in the greater resistance of wooden beams to buckling [57]. Other important data for the commercialization of wood products may be the fiber wall: lumen ratio, primarily because it can be used to predict density [58]. Further, 1-1, 8-1, and 9-1 showed clear advantages relative to the other clones in this trait. In addition, 2-7 had a small MFA, wide vessels, and the highest proportion of axial parenchyma and thus selection of this clone could produce wood suitable for use in manufacturing high-end, value-added products, such as furniture and decorative materials [16]. Knowledge of the intrinsic anatomical characteristics of *C. bungei* as a raw material for solid wood could facilitate the selection of desired traits in future breeding programs.

4.3. Radial Variation in Anatomical Characteristics

There was difference in anatomical characteristics among different cambial ages, indicating that we proved our hypothesis. The ring widths of six *C. bungei* clones were 2–4 rings per cm and these results were consistent with Chinese Catalpa from Yunnan [2]. The annual ring width of *C. bungei* decreased with cambial age [65] and all six clones showed highly similar radial changes, which might be attributed to environmental factors [17,66].

Juvenile wood can be defined as being close to the pith and it differs from mature wood in several ways [20,67]. Maeglin [68] reported shorter fibers with generally thinner walls at or near the pith. Plomion et al. [32] found that juvenile wood often has lower density and larger MFAs. Historical and contemporary studies have identified juvenile and mature wood by density, cell length, MFA, and longitudinal shrinkage [20,42,43,69]. In our study, fiber length and MFA were used to distinguish between juvenile and mature wood. The transition age between juvenile and mature wood was between 7 and 8 years; the width of juveniles ranged between 4.2 and 5.8 cm. These results were similar to those found by Palermo et al. [37], who reported that mature wood occurred between the age of 8 and 13 years. In addition, Ferreira et al. [36] found that the juvenile wood of *Hevea brasiliensis* occurred approximately between 40 and 55 mm from the pith.

According to our results, fiber length, double thickness of cell wall, and the fiber wall: lumen ratio increased significantly with cambial age [30,70,71]. Fiber diameter varied inconsistently radially [39,72]. MFA has generally been found to be below 20° in hardwoods and does not show clear decreasing trends in juvenile and mature wood [73]. Vessel diameters in EW increased rapidly from the pith [74–76]; in LW, vessel diameter was not significantly related with cambial age. The number of vessels decreased with cambial age in EW [71], but in LW there was no radial change. Vessel diameter increased and the number of vessels decreased with cambial age in EW consistent with the porous distribution, which changed from diffuse-porous to semi-ring-porous and then to ring-porous. From the pith to the bark, the porous distribution was also accompanied by decreases in the proportion of fiber and increases in vessel and axial parenchyma proportion; fiber abundance was negatively correlated with both vessel and parenchyma abundance [77].

5. Conclusions

The impacts of the genetic origin on anatomical properties were significant on most of anatomical properties. Radial variations of anatomical properties were distinct. The transition between juvenile and mature wood could be observed between the age of 7 and 8. A similar transition age was observed in the variation curves for other properties such as ring width, double wall thickness in LW, and the fiber wall: lumen ratio. Additional work is needed to characterize the steps that take place during this transition age. Significant differences among clones and patterns of radial variation in anatomical features suggest that care is required in designing selection regimes to obtain wood with desired properties.

Author Contributions: Conceptualization, Y.L., L.Z., and S.L.; methodology, Y.L. and L.Z.; software, Y.L.; validation, Y.L. and Y.Z.; formal analysis, Y.L. and L.Z.; investigation, L.Z. and S.L.; resources, Y.L., L.Z., Y.Z., and S.L.; data curation, Y.L. and Y.Z.; writing—original draft preparation, Y.L.; writing—review and editing, Y.L., L.Z., and S.L.; supervision, S.L.; project administration, L.Z.; funding acquisition, Y.L. and L.Z. All authors have read and agreed to the published version of the manuscript.

Funding: This research was funded by the National Key Research and Development Program of China (No. 2017YFD0600201), and the International Science and Technology Cooperation Program of Anhui Province (1704e1002226).

Acknowledgments: We acknowledge Junhui Wang and Nan Lu for providing trees. We are also grateful for technical assistance from Mengyu Zhou, Shaoqing Wang, Shiliu Zhu, Xinyi Xing, and Gong Rong.

Conflicts of Interest: The authors declare no conflict of interest.

References

1. Olsen, R.T., Jr.; Kirkbride, J.H. Taxonomic revision of the genus Catalpa (Bignoniaceae). *Brittonia* **2017**, *69*, 387–421. [CrossRef]
2. Chen, J.; Yang, J.; Liu, P. *Chinese Timbers*; China Forestry Press: Beijing, China, 1992; pp. 150–152.
3. Ma, W.; Zhang, S.; Wang, J.; Zhai, W.; Cui, Y.; Wang, Q. Timber physical and mechanical properties of new *Catalpa bungei* clones. *Sci. Silvae Sin.* **2013**, *49*, 126–134.
4. Lin, J.; Wu, L.; Liang, J.; Wang, J. Effect of different plant growth regulators on callus induction in *Catalpa bungei*. *Afr. J. Agric. Res.* **2010**, *5*, 2699–2704.
5. Zhang, S.; Wang, J.; Yuan, H.; Ma, J.; Li, Y.; Li, C. Genetic variation in growth, physiological and morphological traits of *Catalpa bungei*. *J. Northeast For. Univ.* **2011**, *39*, 4–8.
6. Zhao, K.; Wang, J.; Jiao, Y.; Yu, J.; Zhao, M. New variety of hybridized Chinese Catalpa-breeding report of Los Chinese catalpa 1, 2. *J. Henan For. Sci. Technol.* **2011**, *31*, 4–6.
7. Ma, W.; Zhang, S.; Wang, J.; Zhang, J.; Zhao, K. Growth traits of one -year -old *Catalpa bungei* clones in seedling stage. *For. Res.* **2012**, *25*, 657–663.
8. Qiu, Q.; Li, J.; Wang, J.; He, Q.; Dong, L.; Ma, J.; Bai, J.; Wu, J. Coupling effects of water and fertilizer on the growth characteristics of *Catalpa bungei* seedlings. *Pak. J. Bot.* **2015**, *47*, 889–896.
9. Qiu, Q.; Wang, J.; Su, Y.; Li, J.; Ma, J.; He, Q. Organ-level evaluation of the carbon starvation hypothesis in deciduous broad-leaved *Catalpa bungei* plants undergoing drought-induced mortality. *Dendrobiology* **2018**, *80*, 48–60. [CrossRef]
10. Tong, B.; Zhao, Y.; Yang, H. Research progress on breeding techniques of Sect. Sino catalpa in northern China. *J. Anhui Agric. Sci.* **2019**, *47*, 1–3, 17.
11. Han, D.; Yang, G.; Xiao, Y.; Wang, Q.; Zhai, W.; Ma, W.; Wang, J.; Wang, L. Study on early growth variation of *Catalpa bungei* clones and optimization. *For. Res.* **2019**, *32*, 96–104.
12. Pérez, D.; Kanninen, M.; Matamoros, F.; Fonseca, W.; Chaves, E. Heartwood, sapwood and bark contents of *Bombacopsis quinata* in Costa Rica. *J. Trop. Sci.* **2004**, *16*, 318–327.
13. Luostarinen, K.; Pikkarainen, L.; Ikonen, V.; Gerendiain, A.Z.; Pulkkinen, P.; Peltola, H. Relationships of wood anatomy with growth and wood density in three Norway spruce clones of Finnish origin. *Can. J. For. Res.* **2017**, *47*, 1184–1192. [CrossRef]
14. Quilho, T.; Pereira, H.; Richter, H.G. Within-tree variation in phloem cell dimensions and proportions in *Eucalyptus globulus*. *Iawa J.* **2000**, *21*, 31–40. [CrossRef]
15. Miranda, I.; Pereira, H. Variation of pulpwood quality with provenances and site in *Eucalyptus globulus*. *Ann. For. Sci.* **2002**, *59*, 283–291. [CrossRef]
16. Huang, C.L.; Lindstrom, H.; Nakada, R.; Ralston, J. Cell wall structure and wood properties determined by acoustics-a selective review. *Holzals Roh-und Werkstoff* **2003**, *61*, 321–335. [CrossRef]
17. Zhang, S.; Belien, E.; Ren, H.; Rossi, S.; Huang, J. Wood anatomy of boreal species in a warming world: A review. *iForest* **2020**, *13*, 130–138. [CrossRef]
18. Doungpet, M. Environment and Genetic Effects on Wood Quality of Populus. Ph.D. Thesis, North Carolina State University, Raleigh, NC, USA, 2005.
19. Šefc, B.; Trajković, J.; Slavko, G.; Padovan, D.; Hasan, M. Selected tree characteristics and wood properties of two poplar clones. *Wood Res. Slovak.* **2009**, *54*, 15–22.
20. Zobel, B.J.; van Buijtenen, J.P. *Wood Variation: Its Causes and Control*; Springer: Berlin, Germany, 1989; pp. 100–119.
21. Ramírez, M.; Rodríguez, J.; Peredo, M.; Valenzuela, S.; Mendonca, R. Wood anatomy and biometric parameters variation of *Eucalyptus globulus* clones. *Wood Sci. Technol.* **2009**, *43*, 131–141. [CrossRef]
22. Guo, L. Research on Variations within Tracheid Traits and Vegetative Propagation Techniques in Chinese Fir Clones. Master's Thesis, Zhejiang A&F University, Zhejiang, China, 2014.
23. Li, R.; Huang, S.; Liang, J.; Zhou, C.; He, C.; Li, L.; Tang, G. Genetic variation of growth traits and wood properties in Chinese fir clones. *J. South. Agric.* **2014**, *45*, 1626–1631.
24. Pande, P.K.; Singh, M. Inter-clonal, intra-clonal, and single tree variations of wood anatomical properties and specific gravity of clonal ramets of *Dalbergia sissoo* Roxb. *Wood Sci. Technol.* **2005**, *39*, 351–366. [CrossRef]
25. Dadswell, H.E. Wood structure variations occurring during tree growth and their influence on properties. *J. Inst. Wood Sci.* **1958**, *1*, 1–24.

26. Butterfield, R.P.; Crook, R.P.; Adams, R.; Morris, R. Radial variation in wood specific gravity, fiber length and vessel area for two central American hardwood: *Hyeronima alchorneoides* and *Vochysia guatemalensis*: Natural and plantation-grown trees. *IAWA J.* **1993**, *14*, 153–161. [CrossRef]
27. Hudson, I.; Wilson, L.; Van Beveren, K. Vessel distribution at two percentage heights from pith to bark in a seven year old *Eucalyptus globulus* tree. *Appita J.* **1997**, *50*, 495–500.
28. Hudson, I.; Wilson, L.; Van Beveren, K. Vessel and fiber property variation in *Eucalyptus globulus* and *Eucalyptus nitens*: Some preliminary results. *IAWA J.* **1998**, *19*, 111–130. [CrossRef]
29. Fan, Z.; Cao, K.; Becker, P. Axial radial variations in xylem anatomy of angiosperm and conifer trees in Yunnan, China. *IAWA J.* **2009**, *30*, 1–13. [CrossRef]
30. Izekor, D.N.; Fuwape, J.A. Variations in the anatomical characteristics of plantation grown *Tectona grandis* wood in Edo State, Nigeria. *Arch. Appl. Sci. Res.* **2011**, *3*, 83–90.
31. Zhao, X. Effects of cambial age and flow path-length on vessel characteristics in birch. *J. Forest Res.-JPN* **2015**, *20*, 175–185. [CrossRef]
32. Plomion, C.; Leprovost, G.; Stokes, A. Wood formation in trees. *Plant Physiol.* **2001**, *127*, 1513–1523. [CrossRef]
33. Bendtsen, B. Properties of wood from improved and intensively managed trees. *For. Prod. J.* **1978**, *28*, 61–72.
34. Loo, J.A.; Tauer, C.G.; McNew, R.W. Genetic variation in the time of transition from juvenile to mature wood in loblolly pine (*Pinus taeda* L.). *Silvae Genet.* **1985**, *34*, 14–19.
35. Zobel, B.J.; Sprague, J.R. *Juvenile Wood in Forest Trees*; Springer: New York, NY, USA, 1998.
36. Ferreira, A.L.; Severo, E.T.D.; Calonego, F.W. Determination of fiber length and juvenile and mature wood zones from *Hevea brasiliensis* trees grown in Brazil. *Eur. J. Wood Wood Prod.* **2011**, *69*, 659–662. [CrossRef]
37. De Palermo, G.P.M.; de Latorraca, J.V.F.; de Carvalho, A.M.; Calonego, F.W.; Severo, E.T.D. Anatomical properties of *Eucalyptus grandis* wood and transition age between the juvenile and mature woods. *Eur. J. Wood Wood Prod.* **2015**, *73*, 775–780. [CrossRef]
38. Ma, J.; Wang, J.; Song, L.; Yun, H. Genetic variation of wood properties of *Catalpa bungei* hybrid clones at the young stage. *J. Northeast For. Univ.* **2014**, *42*, 11–19.
39. Li, S.; Li, X.; Link, R.; Li, R.; Deng, L.; Schuldt, B.; Jiang, X.; Zhao, R.; Zheng, J.; Li, S.; et al. Influence of cambial age and axial height on the spatial patterns of xylem traits in *Catalpa bungei*, a Ring-Porous tree species native to China. *Forests* **2019**, *10*, 662. [CrossRef]
40. Nicholls, J.W.P.; Pederick, L.A. Variation of some wood characteristics of *Eucalyptus nitens*. *Aust. For.* **1979**, *9*, 309–321.
41. Githiomi, J.K.; Dougal, E. Analysis of heartwood–sapwood demarcation methods and variation of sapwood and heartwood within and between 15 year old plantation grown *Eucalyptus regnans*. *Int. J. Appl. Sci. Technol.* **2012**, *2*. Available online: http://197.248.75.118:8282/jspui/handle/123456789/324 (accessed on 28 July 2020).
42. Mansfield, S.D.; Parish, R.; Di Lucca, C.M.; Goudie, J.; Kang, K.; Ott, P. Revisiting the transition between juvenile and mature wood: A comparison of fiber length, microfibril angle and relative wood density in lodgepole pine. *Holzforschung* **2009**, *63*, 449–456. [CrossRef]
43. Gorman, T.M.; Kretschmann, D.E.; Green, D.W.; Wiemann, M.C. Effect of site characteristics on juvenile wood transition in lodgepole pine in the inland northweat. *Wood Fiber. Sci.* **2018**, *50*, 180–192. [CrossRef]
44. Dobrowolska, E.; Wroniszewska, P.; Jankowska, A. Density distribution in wood of European birch (*Betula pendula* Roth.). *Forests* **2020**, *11*, 445. [CrossRef]
45. Cave, I.I. Theory of X—ray measurement of microfibril angle in wood. *For. Prod. J.* **1966**, *16*, 37–42.
46. IAWA, Committee. IAWA list of microscopic features for hardwood identification. *IAWA Bull.* **1989**, *10*, 219–332.
47. Simcha, L.Y.; Paolo, C. Atlas of woody plant stems: Evolution, structure, and environmental modifications. *J. Veg. Sci.* **2008**, *19*, 893–894.
48. Wheeler, E.A.; Baas, P.; Rodgers, S. Variations in dicot wood anatomy: A global analysis based on the inside wood database. *IAWA J.* **2007**, *28*, 229–258. [CrossRef]
49. Helińska-Raczkowska, L. Variation of vessel lumen diameter in radial direction as an indication of the juvenile wood growth in oak (*Quercus petraea* Liebl). *Ann. Des. Sci. For.* **1994**, *51*, 283–290. [CrossRef]
50. Chattaway, M.M. The sapwood-heartwood transition. *Aust. For.* **1952**, 25–34. [CrossRef]
51. Yin, J.; Song, K.; Lu, Y.; Zhao, G.; Yin, Y. Comparison of changes in micropores and mesopores in the wood cell walls of sapwood and heartwood. *Wood Sci. Technol.* **2015**, *49*, 987–1001. [CrossRef]

52. Brito, A.S.; Vidaurre, G.B.; de Oliveira, J.T.S.; Missia Da Silva, J.G.; Rodrigues, B.P.; de Carneiro, A.C.O. Effect of planting spacing in production and permeability of heartwood and sapwood of *Eucalyptus* wood. *Floresta e Ambiente* **2019**, *26*, e20180378. [CrossRef]
53. Kohonen, M.M.; Helland, A. On the function of wall sculpturing in xylem conduits. *J. Bionics Eng.* **2009**, *6*, 324–329. [CrossRef]
54. Wei, L.; McDonald, A.G.; Freitag, C.; Morrell, J.J. Effects of wood fiber esterification on properties, weatherability and biodurability of wood plastic composites. *Polym. Degrad. Stabil.* **2013**, *98*, 1348–1361. [CrossRef]
55. Hein, P.R.G.; Silva, J.R.M.; Brancheriau, L. Correlations among microfibril angle, density, modulus of elasticity, modulus of rupture and shrinkage in 6-year-old *Eucalyptus urophylla x E. Grandis*. *Maderas-Cienc. Tecnol.* **2013**, *15*, 171–182. [CrossRef]
56. Panshin, A.J.; de Zeeuw, C. *Textbook of Wood Technology. Structure, Identification and Uses of The Commercial Woods of the United States and Canada*; McGraw-Hill Book Company: New York, NY, USA, 1980.
57. Van Leeuwen, M.; Hilker, T.; Coops, N.C.; Frazer, G.; Wulder, M.A.; Newnham, G.J.; Culvenor, D.S. Assessment of standing wood and fiber quality using ground and airborne laser scanning: A review. *For. Ecol. Manag.* **2011**, *261*, 1467–1478. [CrossRef]
58. Mitchell, M.D.; Denne, M.P. Variation in density of Picea sitchensis in relation to within-tree trends in tracheid diameter and wall thickness. *Forestry* **1997**, *70*, 47–60. [CrossRef]
59. Hannrup, B.; Danell, O.; Ekberg, I.; Moell, M. Relationships between wood density and tracheid dimensions in *Pinus sylvestris* L. *Wood Fiber Sci.* **2001**, *33*, 173–181.
60. Uprichard, J.M. Wood extracts. In *Primary Wood Processing: Principles and Practice*; Walker, J.C.F., Ed.; Chapman & Hall: London, UK, 1993; pp. 56–63.
61. Yamamoto, H.; Sassus, F.; Ninomiya, M.; Gril, J. A model of anisotropic swelling and shrinking process of wood-Part 2. A simulation of shrinking wood. *Wood Sci. Technol.* **2001**, *35*, 167–181. [CrossRef]
62. Yang, J.L.; Evans, R. Prediction of MOE of eucalypt wood from microfibril angle and density. *Holzals Roh-und Werkstoff* **2003**, *61*, 449–452. [CrossRef]
63. Hein, P.R.G.; Clair, B.; Brancheriau, L.; Chaix, G. Predicting microfibril angle in *Eucalyptus* wood from different wood faces and surface qualities using near infrared spectra. *J. Near Infrared Spec.* **2010**, *18*, 455–464. [CrossRef]
64. Lube, V.; Lazarescu, C.; Mansfield, S.D.; Avramidis, S. Wood microfibril angle variation after drying. *Holzforschung* **2016**, *70*, 485–488. [CrossRef]
65. Garcia-Gonzalez, I.; Souto-Herrero, M.; Campelo, F. Ring-porosity and earlywood vessels: A review on extracting environmental information through time. *IAWA J.* **2016**, *37*, 295–314. [CrossRef]
66. Lenz, P.; Cloutier, A.; MacKay, J.; Beaulieu, J. Genetic control of wood properties in *Picea glauca*: An analysis of trends with cambial age. *Can. J. Forest Res.* **2010**, *40*, 703–715. [CrossRef]
67. Bao, F.; Jiang, Z.; Jiang, X.; Lu, X.X.; Luo, X.; Zhang, S. Differences in wood properties between juvenile wood and mature wood in 10 species grown in China. *Wood Sci. Technol.* **2001**, *35*, 363–375. [CrossRef]
68. Maeglin, R. Juvenile wood, tension wood, and growth stress effects on processing hardwoods. In Proceedings of the 15th annual hardwood symposium of the Hardwood Research Council, Memphis, TN, USA, 10–12 May 1987.
69. Bendtsen, B.A.; Senft, J. Mechanical and anatomical properties in individual growth rings of plantation-grown eastern cotton-wood and loblolly pine. *Wood Fiber Sci.* **1986**, *18*, 23–38.
70. Cardoso, S.; Sousa, V.B.; Quilho, T.; Pereira, H. Anatomical variation of teakwood from unmanaged mature plantations in East Timor. *J. Wood Sci.* **2015**, *61*, 326–333. [CrossRef]
71. Carrillo, I.; Graciela Aguayo, M.; Valenzuela, S.; Teixeira Mendonca, R.; Pedro Elissetche, J. Variations in wood anatomy and fiber biometry of *Eucalyptus globulus* genotypes with different wood density. *Wood Res. Slovak.* **2015**, *60*, 1–10.
72. Istok, I.; Sefc, B.; Hasan, M.; Popovic, G.; Sedlar, T. Fiber characteristics of white poplar (*Populus alba* L.) juvenile wood along the Drava river. *Drv. Ind.* **2017**, *68*, 241–247. [CrossRef]
73. Donaldson, L. Microfibril angle: Measurement, variation and relationships-a review. *IAWA J.* **2008**, *29*, 345–386. [CrossRef]
74. Park, S. Radial variations of elements in the ring-porous wood. *J. Korean Wood Sci. Technol.* **1981**, *9*, 1–6.

75. Peter, G. Implications of anatomical variations in the wood of pedunculate oak (*Quercus Robur* L.), including comparisons with common beech (Fagus Sylvatica L.). *IAWA J.* **1987**, *8*, 149–166.
76. Lei, H.; Milota, M.R. Variation in the anatomy and specific gravity of wood within and between trees of red alder (*Alnus rubra* Bong.). *Wood Fiber Sci.* **1997**, *29*, 10–20.
77. Pratt, R.B.; Jacobsen, A.L. Conflicting demands on angiosperm xylem: Tradeoffs among storage, transport and biomechanics. *Plant Cell Environ.* **2017**, *40*, 897–913. [CrossRef]